AMERICAN JOURNAL OF PHARMTECH RESEARCH

Journal home page: http://www.ajptr.com/

DNA Binding And Cleavage Studies of Isatin Based Pyruvic Acid Derivative and Its Transition Metal Complexes

Divya S. Hegde[1], Kalagouda B. Gudasi[1]*

1. Karnatak University, Pavate Nagar, Dharwad-580 003, Karnataka, India.

ABSTRACT

A novel tridentate chelating ligand, (2Z,2Z)-3,3-dimethyl-2-(2-(2-oxoindolin-3-ylidene)hydrazono)butanoic acid and its Co(II), Ni(II), Cu(II) and Zn(II) complexes were synthesized and characterized by elemental analyses, spectral (vibrational, electronic, ^{1}H NMR, ^{13}C NMR and mass) and thermal studies. The interaction of ligand and complexes with calf-thymus DNA (CT-DNA) has been extensively studied using absorption, emission, viscosity and thermal denaturation studies with *E. coli* DNA. The DNA cleavage ability of ligand and metal complexes were tested using plasmid pBR322 DNA by gel electrophoresis method.

Keywords: Isatin; Pyruvic acid; Transition Metal Complexes; DNA Binding and Cleavage Studies.

*Corresponding Author Email: drkbgudasi@kud.ac.in

Received 14 December 2016, Accepted 20December 2016

Please cite this article as: Gudasi KB *et al.*, DNA Binding And Cleavage Studies of Isatin Based Pyruvic Acid Derivative and Its Transition Metal Complexes. American Journal of PharmTech Research 2017.

INTRODUCTION

The research on development of platinum based metal complexes mainly cisplatin or carboplatin had an enormous impact on cancer chemotherapy. However, the spectrum of cancers that can be treated with platinum based metallo drugs are narrow and caused various side effects and resistance phenomena, hence, general application of these drugs are less advisable now a days. These unresolved problems in platinum-based anti-cancer therapy have stimulated researchers to discover various new drugs with the use of various transition metal ions in the place of platinum with different modes of action than cisplatin. Interestingly, the complexes with iron, cobalt, copper, gold have shown promising results in preclinical studies and compounds with titanium, ruthenium, or gallium central atoms have already been evaluated in phase I and phase II trials.

The anticancer properties of the various compounds are usually carried out in various steps. The preliminary studies include interaction studies of new compounds with Deoxyribonucleic acid (DNA). DNA has information stored in it in the form of genes and these are extremely important for various functions. DNA is the primary target molecule for most anticancer therapies according to cell biology. Investigations on DNA interactions with transition metal complexes, especially for those containing multidentate aromatic ligands, have aroused considerable interests owing to their potential applications as new therapeutic agents and interesting properties that make them as possible probes of DNA structure and conformation[1].Considering these, we planned for the syntheses of late transition metal complexes with known pyruvic acid based newly derived organic ligand.

Pyruvic acid ($CH_3COCOOH$) is the simplest of the alpha-keto acids, consisting of carboxylic acid and a ketone functional group. Pyruvate (CH_3COCOO^-) the anionic form of a pyruvic acid, involves in the intermediary metabolism process as a product of glycolysis. Several clinical tests proved that, pyruvic acid and its derivatives are good anticancer agents. Substituted hydrazones of pyruvate derivatives and their transition metal associates are capable of interacting with specific conformations of DNA double helix or with specific DNA base sequences, and eventually to induce apoptosis. Redox activeness of first row transition metal ions in the ligand periphery reflects their ability to cleave DNA in the oxidative process. Hence functions of DNA will alter and may reduce the rapid cell growth in cancer infected cells.

Isatin, 1H-indole-2,3-dione is an versatile chemical building block, able to form a large number of heterocyclic molecules. In terms of its mode of action, isatin is proposed to inhibit cancer cell proliferation via interaction with extracelleuar signal related protein kinases and thereby promoting

apoptosis. Isatin derivatives widely present endogenously in both human and other mammalian tissues and fluids likely as a result of the tryptophan metabolic pathway. The versatility of isatin's molecular architecture makes it an ideal platform for structural modification and derivatization as evidenced by the fact that many isatin derivatives exhibit a broad range of biological activities such as anticancer [2,3], antidepressant [4], anticonvulsant [5], antifungal [6], anti-HIV [7] and anti-inflammatory [8], etc. In the last several decades, increasing numbers of researchers from both industry and academia have embarked on the development of new isatin-based anticancer agents [9]. Considering the various applications of indole and pyruvic in medicinal field, we have synthesized new derivative containing heterocyclic indole ring and pyruvic acid moiety to obtain combined activity of both. The new ligand is treated with various transition metal ions to get desired metal complexes. The synthesized compounds were screened for DNA binding and cleavage studies as preliminary test of anticancer activity.

MATERIALS AND METHOD

All the solvents and metal chlorides used are of AR grade. Isatin, tris-base and tris-HCl and ethidium bromide (EB) were obtained from Sigma Aldrich and were of analytical grade. Trimethyl pyruvic acid is obtained from Alfa Aeser. Hydrazine hydrate and metal chlorides were obtained from Spectrochem, India. Calf thymus DNA was procured from SRL, India. Plasmid DNA-pBR322 was purchased from Chromous Biotech, India. Agarose was obtained from Lonza (India). All the solvents were obtained from S.D. Fine chemicals.

Metal determination for Co(II), Ni(II) and Cu(II) complexes was determined volumetrically and that of Zn(II) complex gravimetrically as per literature procedure. Conductance measurements were recorded in DMF (10^{-3} M) using ELICO-CM-82 conductivity bridge with cell type CC-01 and cell constant 0.53. The IR spectra were recorded on a Nicolet 170SX FT-IR spectrometer with the fixed range of 4000-400 cm^{-1} using KBr disks. Elements such as carbon, hydrogen and nitrogen were determined using Thermo quest elemental analyzer. ^{1}H and ^{13}C NMR spectra of ligand and zinc complex were recorded in DMSO-d_6 on a Bruker 500 MHz spectrometer. Electronic spectra were recorded on a Hitachi-U-3310 UV-visible spectrophotometer in the 200-800 nm range using DMF (10^{-3} M) as the solvent. Thermogravimetric studies were carried out over a temperature range of 25-1000°C using TGAQ500 analyzer with a heating rate of 10°C min^{-1}.

SYNTHESIS

Preparation of the Ligand

The ligand was synthesized in two+ simple steps and synthetic route is presented in **Scheme 1**. All

the intermediates are characterised by NMR and GC mass analyses. The synthesis ligand is briefly described below.

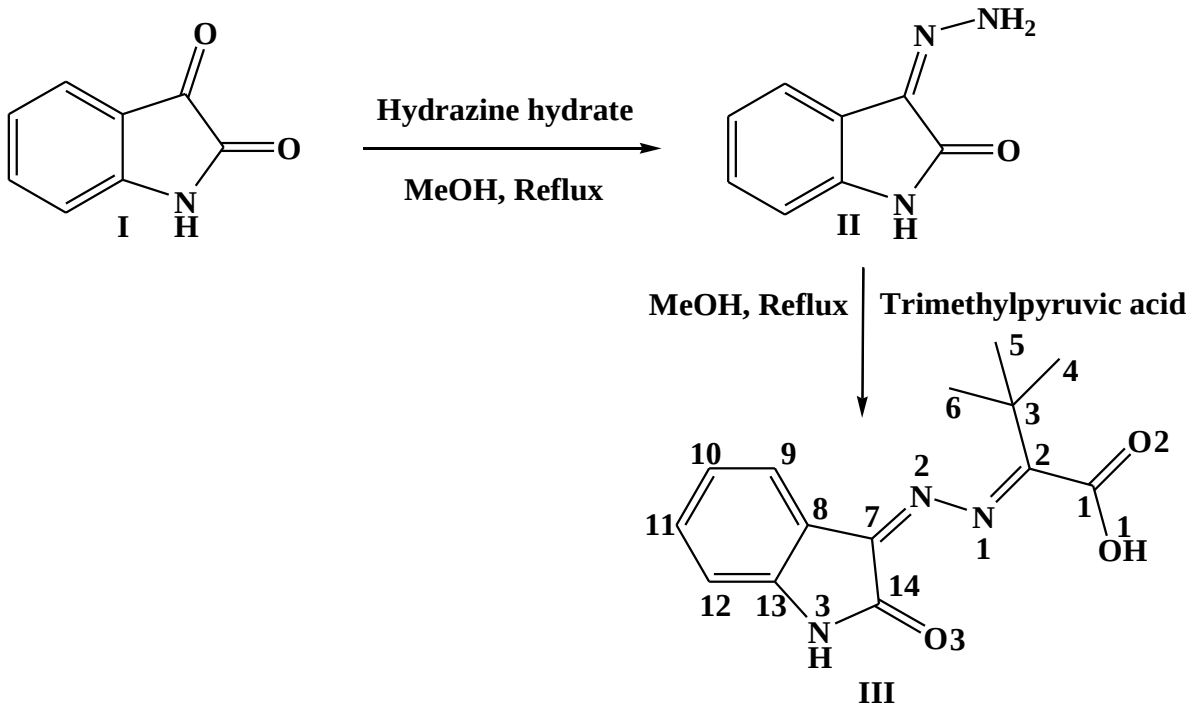

Scheme 1. Synthetic route for Ligand

Synthesis of 3-hydrazinylindol-2-one (II)

The Hydrazine hydrate (15.01g, 3mM) was added to methanolic solution (20 mL) of isatin (14.71 g, 100mM) under stirring and resulting solution was refluxed for 3 h and then cooled to room temperature, until a yellow solid separates. The resultant solid was filtered, washed with ethanol and dried in air and recrystallised from methanol. The purity of the compound was checked by TLC on pre-coated silica gel plates. Yield: 90 %.

Synthesis of (2Z,2Z)-3,3-dimethyl-2-(2-(2-oxoindolin-3-ylidene)hydrazono)butanoic acid (III)

Trimethylpyruvic acid (8.07g, 100 mM) was added to methanoilc (20 mL) solution of 3-hydrazinylindol-2-one (10.00g, 100mM) under stirring and refluxed for 3h. The yellowish orange solid separated was filtered, washed with ethanol and dried under vacuum and recrystallized from methanol. (Rf:0.45, solvent mixture; chloroform: Ethyl acetate, 1:1). Yield: 75%, M.P. 340ºC.

Preparation of the complexes

Synthesis of Co(II), Ni(II), Cu(II) and Zn(II) complexes

The ligand, (2Z,2Z)-3,3-dimethyl-2-(2-(2-oxoindolin-3-ylidene)hydrazono)butanoic acid (0.5g, 1 mM) was dissolved in minimum quantity of methanol, and to which, an aqueous methanolic solution of Co(II), Ni(II), Cu(II), Zn(II) metal chlorides (1mM) were added separately. The

reaction mixtures were stirred for 6-7 hrs at room temperature to obtain respective complexes. After completion of the reaction, the precipitate obtained was filtered, washed with methanol followed by ether and air dried.

DNA Interaction Studies

Absorption, viscosity and emission experiments involving the binding of compounds with CT-DNA were carried out in a doubly distilled water buffer with tris(hydroxymethyl)aminomethane (Tris, 5 mM) and sodium chloride (50 mM) and adjusted to pH 7.2 with hydrochloric acid. A solution of CT-DNA in the buffer gave a ratio of UV absorbance of about 1.8–1.9 at 260 and 280 nm. The CT-DNA concentration per nucleotide was determined spectrophotometrically by employing an extinction coefficient of 6600 dm^3mol^{-1} cm^{-1} at 260 nm. Absorption titration experiments were performed by maintaining a constant ligand and metal complex concentration (20 μM) and varying DNA concentration (0-60 μM) in buffer. While measuring the absorption spectra, an equal amount of DNA was added to both the test solution and the reference solution to eliminate the absorbance of DNA itself. After addition of DNA to the ligand and metal complex, the resulting solution was allowed to equilibrate at 25ºC for 20 min, after which absorption readings were noted. The data were then fit to following equation **(1)** to obtain intrinsic binding constant Kb [10,11].

$$\mathbf{[DNA]/[\varepsilon_a - \varepsilon_f] = [DNA]/[\varepsilon_b - \varepsilon_f] + 1/Kb[\varepsilon_b - \varepsilon_f]} \quad \mathbf{(1)}$$

Where, [DNA] = concentration of DNA in base pairs,

ε_a= is the extinction coefficient observed for the MLCT absorption band at the given DNA concentration,

ε_f= is the extinction coefficient of the complex without DNA, and

ε_b= is the extinction coefficient of the complex when fully bound to DNA.

A plot of $[DNA]/[\varepsilon_a - \varepsilon_f]$ versus [DNA] gave a slope $1/[\varepsilon_a - \varepsilon_f]$ and intercept equal to $(1/Kb)[\varepsilon_b - \varepsilon_f]$. The intrinsic binding constant Kb is the ratio of slope to the intercept.

Viscosity experiments were carried out using Ostwald microviscometer maintained at 26ºC in a thermostatic water bath maintained at 25 ^oC. DNA samples with approximately 200 base pairs in length were prepared by sonication in order to minimize the complexities arising from DNA flexibility. Titrations were performed by addition of a small volume of concentrated stock solutions of ligand and complexes to a solution of calf thymus DNA in the viscometer. Flow times were observed with a digital stopwatch; each sample was measured three times and average flow time was calculated. Flow time of solutions in phosphate buffer was recorded in triplicate and an

average flow time was calculated. Data were presented as $(\eta/\eta^0)^{1/3}$ versus binding ratio, where η is the viscosity of DNA in the presence of complex and η^0 is the viscosity of DNA alone [10, 12, 13].

The apparent binding constants (Kapp) of the complexes were determined by fluorescence spectral technique using ethidiumbromide (EtBr) bound CT-DNA solution in phosphate buffer. The changes in fluorescence intensities at 596nm (546 nm excitation) of EtBr bound to DNA were recorded with an increasing amount of ligand and metal complex concentration. EtBr was non-emissive in phosphate buffer due to fluorescence quenching of the free EtBr by the solvent molecules [10, 11, 13]. Addition of a second DNA binding molecule would quench the EtBr emission by either replacing the DNA-bound EtBr (if it binds to DNA more strongly than EtBr) or accepting an excited state electron from EtBr. The apparent binding constant (Kapp) has been calculated from the equation **(2)** [14].

$$\mathbf{K_{EtBr}[EtBr]=K_{app}[Compound]} \quad \mathbf{(2)}$$

Where, K[EtBr] is 1 $x10^7M^{-1}$ and the concentration of EtBr is 20 μM; [compound] is the concentration of the compound causing 50% reduction in the emission intensity of EtBr.

DNA Melting Experiments

DNA melting experiments were carried out in phosphate buffer on a HITACHI U-3310 spectrophotometer equipped with a temperature-controlling programmer ETC-717 (5ºC). Solutions of *E. coli* DNA (*Escherichia coli* DNA) in phosphate buffer gave a ratio of UV absorbance at 260 and 280nm (A260/A280) as 1.8-1.9, indicating that the DNA was pure and sufficiently free of contaminants like the proteins and RNA. UV melting profiles were obtained by scanning A260 absorbance monitored at a heating rate of 5ºC /min for solutions of *E. coli* DNA (100 μM) in the absence and presence of ligand and metal complexes (20 μM) from 25 to 85ºC. The melting temperature T_m, which is defined as the temperature where half of the total base pairs are unbound, was determined from the midpoint of the melting curves [15].

DNA Cleavage Studies

The DNA cleavage study of the synthesized compounds was determined by agarose gel electrophoresis using the *E. coli* pBR322 plasmid as a target. The synthesized compounds (100μM) were dissolved in 6 % DMSO (dimethylsulfoxide) solvent and mixed with the target plasmid (1:1). The mixture was then incubated at 37ºC for 2 h. After the incubation period, the plasmid and the compound mixture was mixed with the tracking dye bromophenol blue (1:1). It was then loaded into 1% agarose gel (containing 0.5 μg/mL ethidium bromide) wells along with two control wells, the first one with the untreated plasmid and the second one with the plasmid treated with DMSO solvent. Finally it was electrophoresed at 50 V constant voltage for about 30

mins using Tris-EDTA (TAE) buffer [10-13]. The bands were visualized by UV light and photographed for analysis. The extent of cleavage of the supercoiled DNA was determined by measuring intensities of the bands using Molecular Imager Geldoc gel-XR imaging system (BIORAD).

RESULTS AND DISCUSSION

Analytical and spectroscopic data for the ligands and their complexes indicate 1:1 metal–ligand stoichiometry for all the complexes. The ligand is soluble in chloroform, hot methanol, DMF and DMSO and complexes in DMF and DMSO. The complexes are non-hygroscopic and stable in both solid and solution phases. The molar conductance values are too low for all the complexes in DMF, suggesting their non-electrolytic nature. The analytical and physico-chemical parameters of ligands and complexes are compiled in **Table 1.** Elemental and metal determination data's are in good agreement with proposed structures for the complexes.

Table 1: Analytical, conductance and electronic spectral data

Code	Empirical formula	Elemental analysis (%) found (calculated)					Conductance $Ohm^{-1} mol^{-1} cm^2$	λ_{max} nm
		C	H	N	Cl	M		
LH	$C_{14}H_{15}N_3O_3$	61.47(61.53)	5.36(5.53)	15.32(15.38)	--	--	4.8	340, 364, 407
CoL	$[Co(C_{14}H_{13}N_3O_3)(H_2O)_3].H_2O$	41.74(41.80)	5.21(5.26)	10.42(10.45)	--	14.54(14.65)	2.2	340, 524
NiL	$[Ni(C_{14}H_{14}N_3O_3)\ Cl(H_2O)_2].H_2O$	39.84(39.99)	4.81(4.79)	9.87(9.99)	8.38(8.43)	13.87(13.96)	1.9	387, 430, 570
CuL	$[Cu(C_{14}H_{14}N_3O_3)\ Cl(H_2O)_2].H_2O$	39.30(39.53)	4.59(4.74)	9.71(9.88)	8.27(8.34)	14.57(14.94)	3.3	361, 780
ZnL	$[Zn\ (C_{14}H_{14}N_3O_3)\ Cl(H_2O)_2]$	40.98(41.10)	4.36(4.43)	10.14(10.27)	8.54(8.66)	15.94(15.98)	2.8	--

Table 2: Diagnostic IR bands (cm^{-1}) of ligand and its metal complexes

Comp. Code	υ (C14=O3)	υ (C1=O2)	υ (COO^-) asym	υ (COO^-) sym	υ(C2=N1)	υ(C7=N2)	New υ(C=N)	υ(N3H)	υ(O1H)
LH	1721	1702	--	--	1610	1615	--	3276	3438
CoL	--	--	1604	1355	1591	1614	1620	--	--
NiL	1662	--	1609	1361	1573	1610	--	3139	--
CuL	1648	--	1598	1364	1577	1618	--	3140	--
ZnL	1650	--	1603	1359	1592	1615	--	3278	--

Infrared spectral studies

The diagnostic IR bands of ligand and its complexes are compiled in Table 2. IR spectrum of hydrazone ligand exhibit a medium intensity bands at 3438 cm^{-1} and 3276 cm^{-1} are assigned to ν(O1H) and ν(N1H) respectively. Another two strong signals at appeared at 1721 and 1702 cm^{-1} were assigned to isatin carbonyl ν(>C14=O3) and acid carbonyl ν(>C1=O2) respectively. The medium intensity sharp signal appeared at 1610 and 1615 cm^{-1} were assigned to ν(C2=N1) and ν(C7=N2) respectively.

On complex formation, the signal corresponds to ν(>C1=O2) was disappeared in all complexes, and simultaneously two new bands were appeared in the range of 1598-1609 cm^{-1} and 1355-1364 cm^{-1}, and were assigned to asymmetric and symmetric stretching frequencies of coordinated carboxylate ion in unidentate fashion. The signal corresponds to isatin carbonyl ν(>C14=O3) was shifted to lower frequencies in case of Cu(II), Ni(II), Zn(II) complexes indicates its involvement in coordination. The signal for ν(>C14=O3) was found at 1721 cm^{-1} was disappeared on formation of Co(II) complex, this indicates the involvement of C14=O3 functional group in coordination with metal ion via enolisation followed by deprotonation. This coordination was further confirmed by appearance of new signal at 1620 cm^{-1}, in Co(II) complex, which corresponds to formation of new functional group (C=N).

The broad band at 3438 cm^{-1} in the ligand spectrum correspond to ν(O1H) was absent in the spectra of all metal complexes, suggesting its involvement in coordination via deprotonation. This was further supported by the absence of the signal corresponding to O1H in the ^{1}H NMR spectrum of zinc complex. The signal corresponds to ν(N1H) was disappeared in Co(II) complex and shifted to higher frequencies in rest of the complexes. This suggests the enolisation of N1H with adjacent C=O group and followed by deprotonated in case of Co(II) complex and not in rest of the complexes.

The presence of lattice held and/or coordinated water molecules are confirmed by the appearance of a weak non-ligand band in the region 804-887cm^{-1} assignable to rocking mode of coordinated/lattice held water molecule in all the complexes [16]. This was further confirmed by thermogravimetric analysis.

NMR studies

The numbering scheme followed for the NMR assignment of carbons and protons is presented in Scheme 1. The ^{1}H and ^{13}C NMR spectral assignments of the ligand and its Zn(II) complex are compiled in Table 3. The ^{1}H and ^{13}C NMR spectra of ligand are presented in Figures 1-2 and those of Zn (II) complex in Figures 3-4.

Table 3: ^{1}H and ^{13}C NMR spectral data for ligand and its Zinc complex (shifts in ppm)

Position	Ligand		Zn-Complex	
	^{1}H-NMR	^{13}C-NMR	^{1}H-NMR	^{13}C NMR
C1	--	163.42	--	167.51
C2	--	144.73	--	153.25
C3	--	42.00	--	42.33
C4	2.494	25.24	2.512	25.03
C5	2.490	25.24	2.506	25.03
C6	2.484	25.24	2.596	25.03
C7	--	134.42	--	139.08
C8	--	115.77	--	115.55
C9	7.415-7.397 (d,1H)	128.20	7.422-7.409(d,1H)	129.41
C10	6.995-6.899 (d,1H)	122.75	7.122-7.114(d,1H)	122.08
C11	7.026-7.009 (d,1H)	133.59	7.288-7.254(d,1H)	133.98
C12	7.506-7.491 (d,1H)	122.56	7.586-7.568(d,1H)	122.96
C13	--	144.34	--	144.78
C14	--	145.19	--	149.21
N3H	10.92 (s,1H)	--	11.50(s,1H)	--
O1H	10.99 (s,1H)	--	--	--

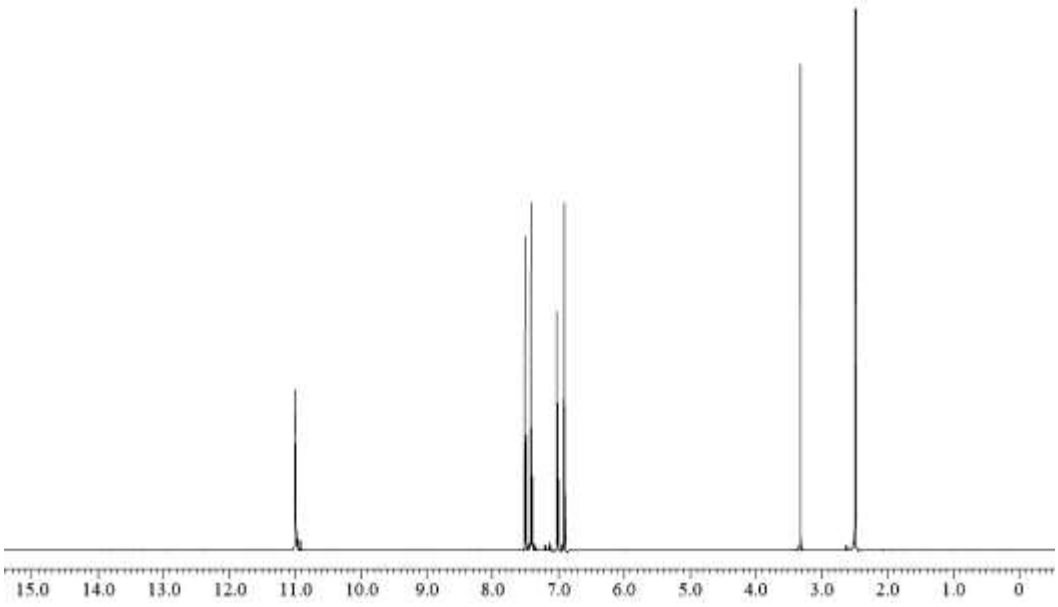

Figure 1: ^{1}H NMR spectrum of LH

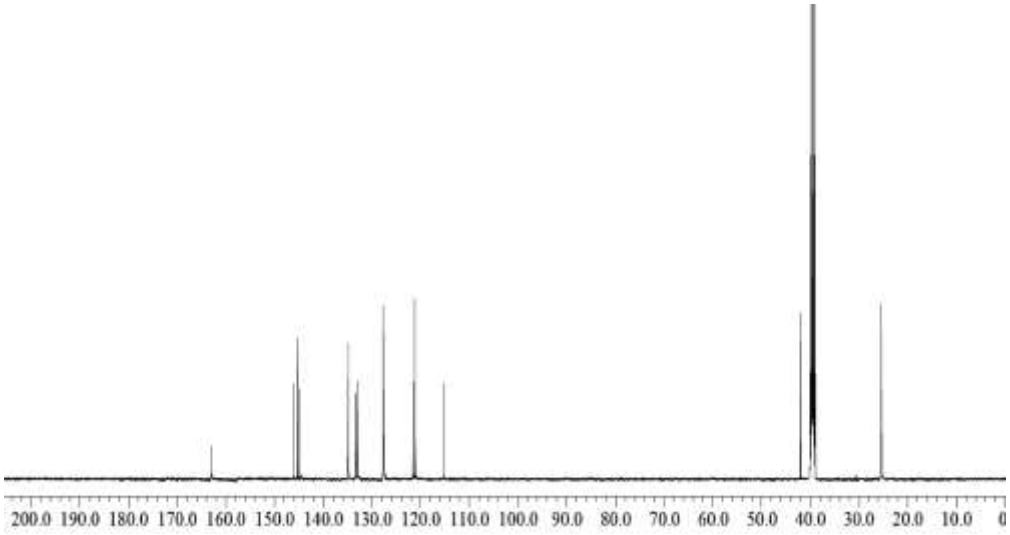

Figure 2: ^{13}C NMR spectrum of LH

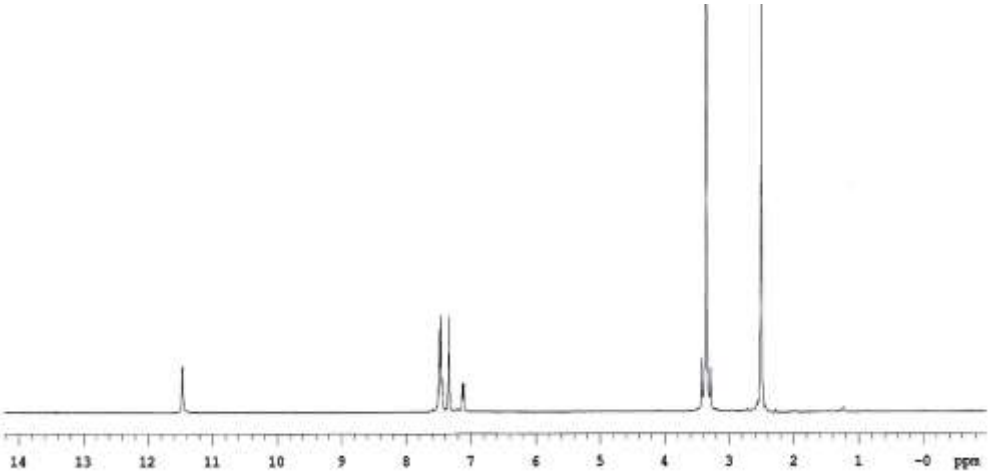

Figure 3:^{1}H NMR spectrum of ZnL

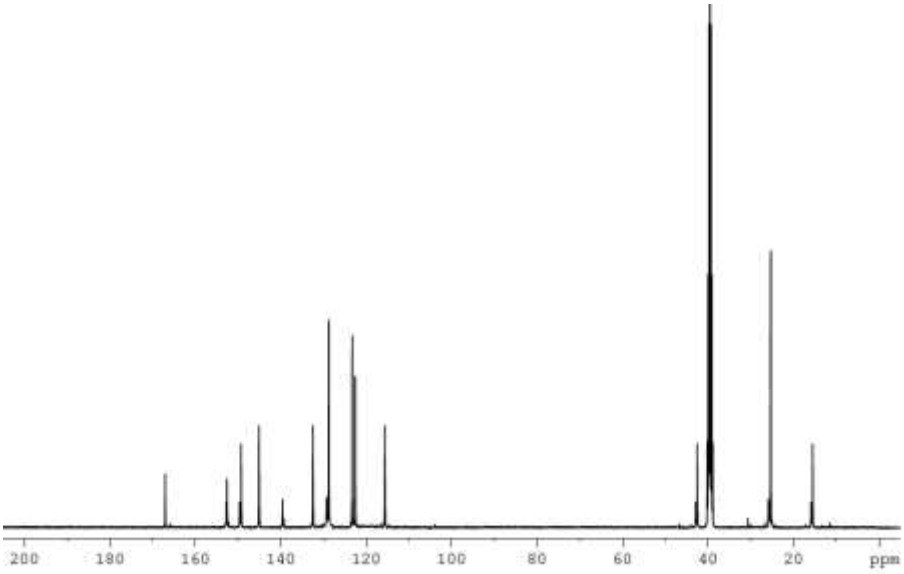

Figure 4: ^{13}C NMR spectrum of ZnL

NMR experiments confirm the structures of the synthesized ligand and its Zn(II) complex. The ^{1}H NMR of ligand exhibits two singlet's at 10.99 and 10.92 ppm are assigned to O1H and N3H protons respectively [17]. On complex formation, the signal corresponds to OH was disappeared suggest that, coordination of OH group via deprotonation. The signals for methyl groups are observed in the range of 2.00 to 2.49 ppm and these have shown slight shift on formation of complex. The aromatic protons were observed in the range of 6.89 to 7.50 ppm in ligand and are shifted to 7.00 to 7.68 ppm on complexation suggests the involvement of ligand in complex formation.

The ^{13}C NMR of ligand and Zn(II) complex are in accordance of proposed structure. The signals due to C1 (163.42 ppm) and C14 (145.19 ppm) in ligand spectrum were shifted to 167.51 and 149.21 ppm on formation of zinc complex indicates the participation of carboxylate oxygen and isatin carbonyl oxygen in coordination respectively. The signal due to C2 appeared at 144.73 ppm in the ligand spectrum has shifted to 153.25 ppm on complexation, indicating involvement of azomethine nitrogen (N1) in the coordination. The aromatic carbons in the ligand spectrum were observed in the range of 122.75 to 145.19 ppm and were shifted to 122.08 to 149.21 ppm on complex formation. The aliphatic carbons were also suffered minimum shift on formation of complex.

It is evident from IR, ^{1}H NMR and ^{13}C NMR spectra of zinc complex that the ligand coordinates through carboxylate oxygen in unidentate fashion, isatin carbonyl oxygen and azomethine nitrogen towards zinc (II) ion.

Electronic Spectral Studies

The electronic absorption spectrum of ligand exhibit strong bands at around 301, 364 and 407 nm respectively assignable to $\pi \rightarrow \pi^*$, $n \rightarrow \pi^*$ transitions associated with azomethine linkage 18, 19. All the complexes show $\pi \rightarrow \pi^*$ transition in the range 340-387 nm. Electronic spectrum of cobalt complex shows a d–d transition around 524 nm assigned to $^{4}T_{1g}(F) \rightarrow {}^{4}T_{1g}(P)$ transition, which is consistent with an octahedral geometry. Ni(II) complex the bands near 570 and 430 nm were assigned to $^{3}A_{2g} \rightarrow {}^{3}T_{1g}$ and $^{3}A_{2g} \rightarrow {}^{3}T_{1g}(P)$ respectively, indicating an octahedral geometry around Ni(II) ion [19, 20]. A broad band around 780 nm appearing as an envelope in the Cu(II) complex, was assigned to $^{2}Eg \rightarrow {}^{2}T_{2g}$ transition which reveals the octahedral geometry [18-21]. The electronic spectra of Nickel complex is depicted in the Figure 5 as a representative.

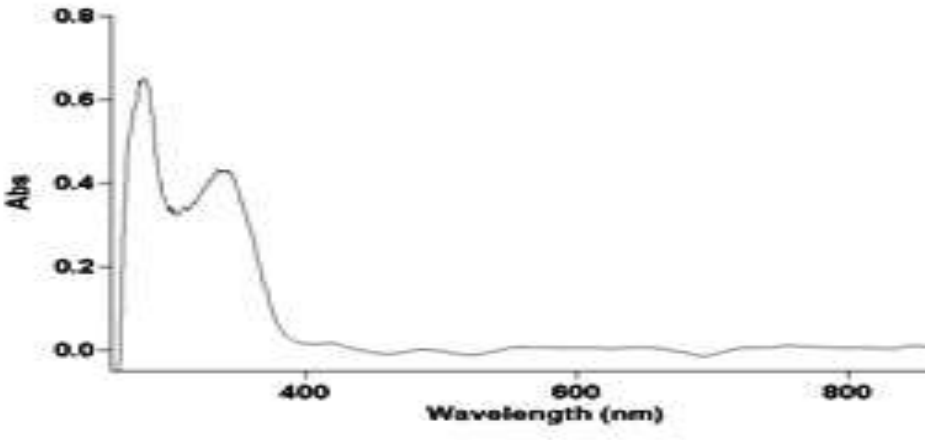

Figure 5: UV-Visible spectrum of NiL

Mass Spectral Analyses

The EI-mass spectra of $C_{14}H_{15}N_3O_3$, $[Co(C_{14}H_{13}N_3O_3)(H_2O)_3].H_2O$, $[Ni(C_{14}H_{14}N_3O_3)Cl(H_2O)_2].H_2O$, $[Cu(C_{14}H_{14}N_3O_3)Cl(H_2O)_2].H_2O$, and $[Zn(C_{14}H_{14}N_3O_3)Cl(H_2O)_2]$ have been recorded and representative spectra are presented in Figure 6 and 7. The ESI mass spectra of cobalt, nickel, copper and zinc complexes show molecular ion peaks at m/z $402(M-1)^+$, $420(M+2)^+$, $426(M+1)^+$ and $407(M-2)^+$ which correspond to their respective molecular weights.

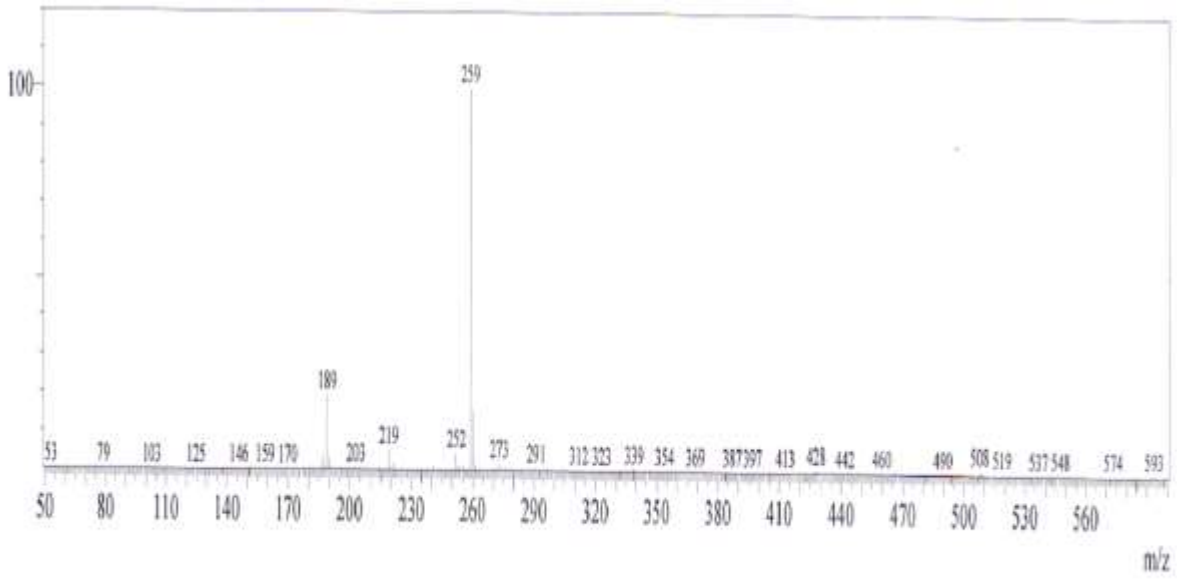

Figure 6: Mass spectrum of LH

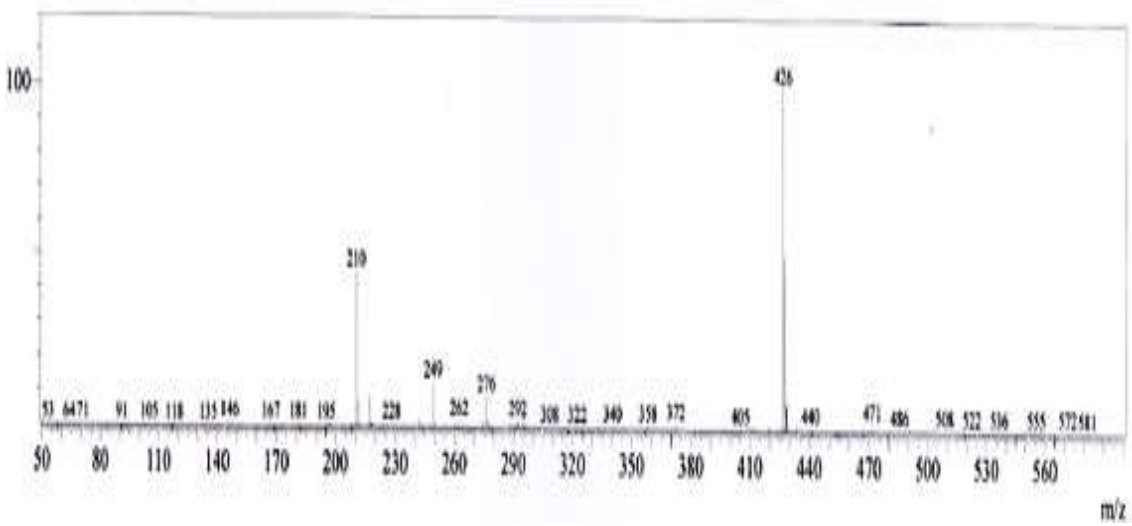

Figure 7: ESI Mass spectrum of CuL

Thermal Analyses

In order to understand the thermal stability and decomposition pattern, we have undertaken the thermo-gravimetric analyses for all synthesized complexes in the temperature range 25-1000ºC. The representative thermogram of Co(II) complex was presented in Figure 8. All the complexes except Zn(II) complex exhibit a weight loss in the temperature range of 79 to 112 ºC indicating the presence of lattice held water. The Co(II), Ni(II) and Cu(II) complexes shown weight loss of 4.01%, 4.34% and 3.98 % respectively in the temperature between 89-109ºC, 85-110ºC and 92-112ºC respectively, which indicates presence of one lattice held water molecule in each metal complexes [22]. The loss of lattice held water molecule is followed by loss of coordinated water molecules in the temperature range 109-181ºC, 110-165ºC, 112-175ºC, and 137-187 for Co(II), Ni(II), Cu(II) and Zn(II) complexes respectively. In case of Ni(II), Cu(II) and Zn(II) complexes, weight loss of 8.14%, 8.52% and 8.54 % were observed respectively in the temperature range of 165-220ºC, 175-241ºC and 137-187ºC respectively assignable to loss of one coordinated chloride ion in each complexes.

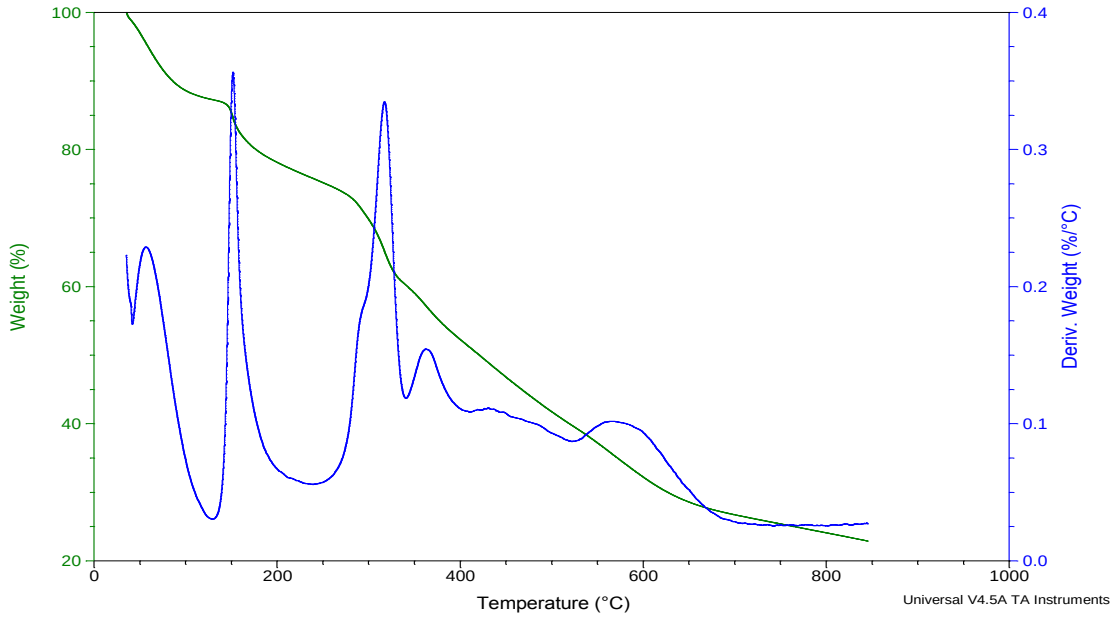

Figure 8: Thermogram of CoL

Table 4: Thermal decomposition details of the complexes

Comp.	Temp. range	Weight loss in %		Weight loss due to
		Found	Calc.	
CoL	79-109	4.01	4.47	One lattice held water molecule
	109-181	13.12	13.42	Three coordinated water
	181-792	67.89	67.43	One ligand
	792-1000	14.99	14.68	Metal residue
NiL	85-110	4.34	4.28	One lattice held water molecule
	110-165	8.14	8.56	Two coordinated water molecules
	165-220	8.12	8.43	One coordinated chloride ion
	220-798	64.47	64.75	One ligand
	798-1000	14.93	13.98	Metal residue
CuL	92-112	3.98	4.23	One lattice held water molecule
	112-175	8.52	8.46	Two coordinated water molecules
	175-241	8.27	8.33	One coordinated chloride ion
	241-787	64.19	64.02	One ligand
	787-1000	15.04	14.96	Metal residue
ZnL	137-187	8.87	8.79	Two coordinated water molecules
	187-240	8.54	8.65	One coordinated chloride ion
	240-778	66.34	66.49	One ligand
	778-1000	16.25	16.07	Metal residue

Thermogram of each metal complexes exhibited the loss of one coordinated ligand molecules in the temperature range of 181-792ºC, 220-798ºC, 241-787ºC and 240-778ºC for Co(II), Ni(II), Cu(II) and Zn(II) complexes respectively. The calculated and observed weight losses are in good agreement with proposed structures. The weight loss after the loss of ligand in all complexes was considered as the formation of metal residues.

DNA Interaction Studies

Absorption Spectral Studies

Examining the changes in absorption spectrum of the metal complexes upon addition of increasing amounts of DNA is one of the most widely used methods to know the interaction of metal complexes with DNA and for determining overall binding constants. The absorption spectra of ligand and complexes in the presence and absence of CT-DNA is shown in the Figure 9. Compound bound to DNA through intercalation usually results in hypochromic effect and red shift (bathochromic effect). The extent of the hypochromism is commonly consistent with the strength of intercalative interaction. Upon addition of calf-thymus DNA to ligand and its complexes, there is a decrease in molar absorptivity (hypochromism) of the intense intraligand absorption bands (240-400 nm) of complexes. The hypochromism in case of ligand (310 nm), cobalt complex (320 nm), nickel complex (390 nm), copper complex (365 nm) and zinc complex (315nm) indicate strong binding with DNA. In order to compare the DNA-binding affinities of these complexes quantitatively, their intrinsic binding constants with CT-DNA is obtained by monitoring the changes in absorption at intraligand band with increasing concentrations of DNA using equation (1) and is found to be $1.18 \times 10^4\ M^{-1}$, $0.32 \times 10^4\ M^{-1}$, $0.23 \times 10^4\ M^{-1}$, $2.48 \times 10^4\ M^{-1}$, $0.95 \times 10^4\ M^{-1}$ and $0.26 \times 10^4\ M^{-1}$ for ligand, cobalt, nickel, copper and zinc complexes respectively. This indicates copper complex shows strong binding to DNA compare to ligand and other compounds which shows weaker interaction.

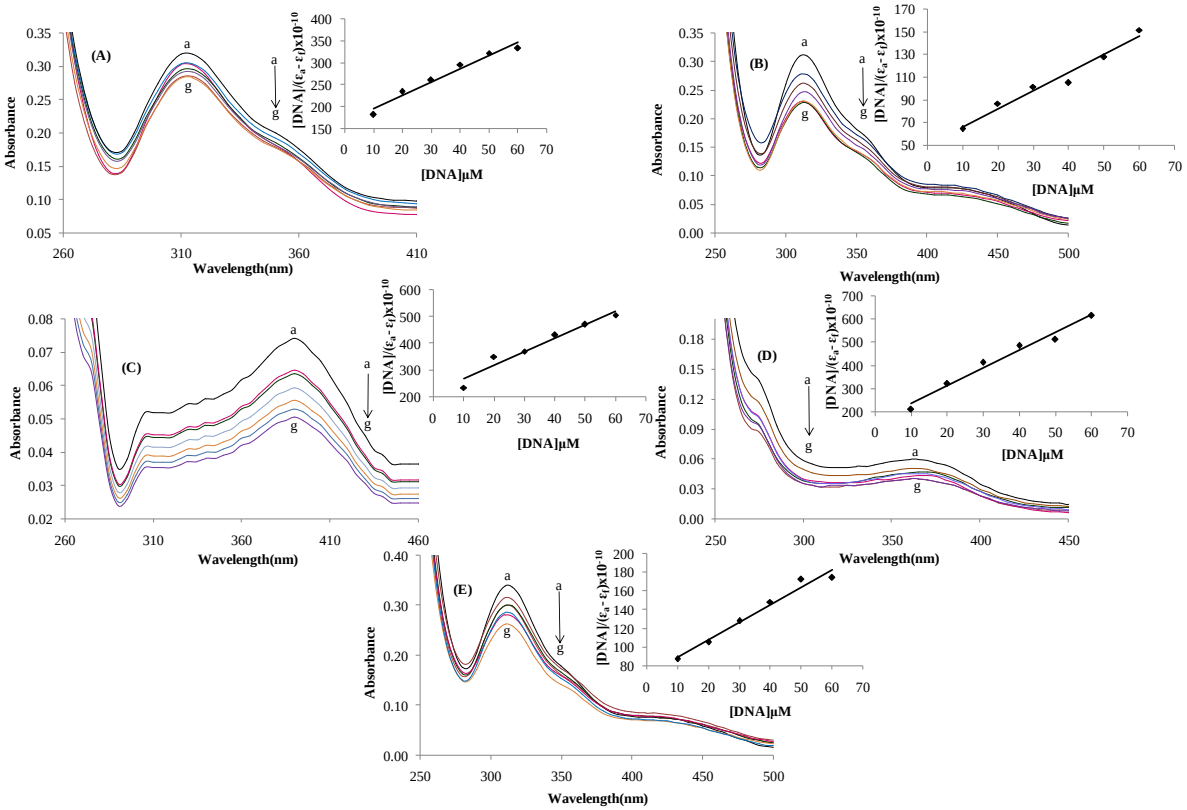

Figure 9: Electronic absorption spectra of LH(A), CoL(B), NiL(C), CuL(D) and ZnL(E) (20uM) with increasing concentrations (0-50uM) of CTDNA (phosphate buffer, pH=7.2); the inset shows a fitting of the absorbance data at 310, 320, 390, 365 and 315 nm for LH, CoL, NiL, CuL and ZnL respectively, used to obtain binding constants.

DNA Thermal Denaturation

Interacalation of small molecules into the double helix is known to increase the helix melting temperature (Tm), the temperature at which the double helix denatures into single-stranded DNA. The extinction coefficient of DNA bases at 260 nm in the double strand is much less than that in the single-stranded form. Hence, melting of the helix leads to an increase in the absorption at this wavelength. *E. coli* DNA was seen to melt at 55-60ºC (phosphate buffer) in the absence of complex [14]. The melting temperature of DNA on addition of ligand and zinc complex is found to be in the region 60-65ºC for cobalt and nickel complex it is found in the range 65-70ºC and for copper complex it is found in the range 70-75ºC which indicates that copper complex binds strongly compared to other compounds tested (Figure 10). This behavior is comparable to classical intercalators.

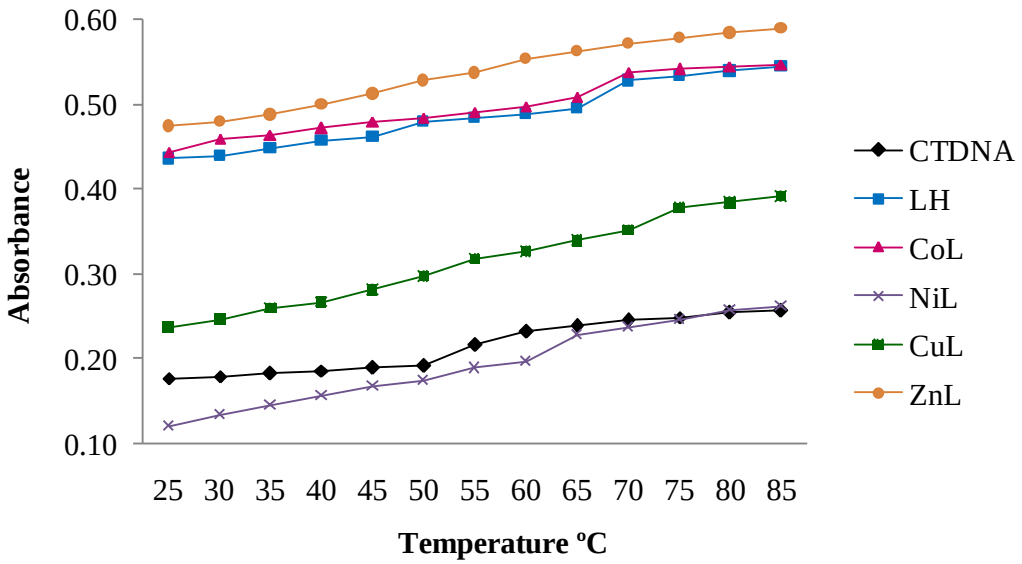

Figure 10: Melting curves of CT-DNA in the absence and presence of LH, CoL, NiL, CuL and ZnL.

Ethidium Bromide Displacement Assay

The competitive DNA binding of complexes has been studied by examining changes in emission intensity of ethidium bromide (EtBr) bound to CT-DNA as a function of the concentration of complexes added. Though the emission intensity of EtBr in buffer medium is quenched by the solvent molecules, it is enhanced by its stacking interaction between adjacent DNA base pairs. Ligand and complexes when added to DNA pretreated with EtBr {[DNA]/[EtBr]=1:1}, the DNA-induced emission intensity of EtBr has decreased as shown in Figure 11. The Kapp values for cobalt, copper and iron complexes are $20x10^6$ M^{-1}, for ligand and zinc complex are $10x10^6$ M^{-1} and for nickel complex is $6.6x10^6$ M^{-1}. The higher values of Kapp indicate that these compounds bind to DNA by intercalation.

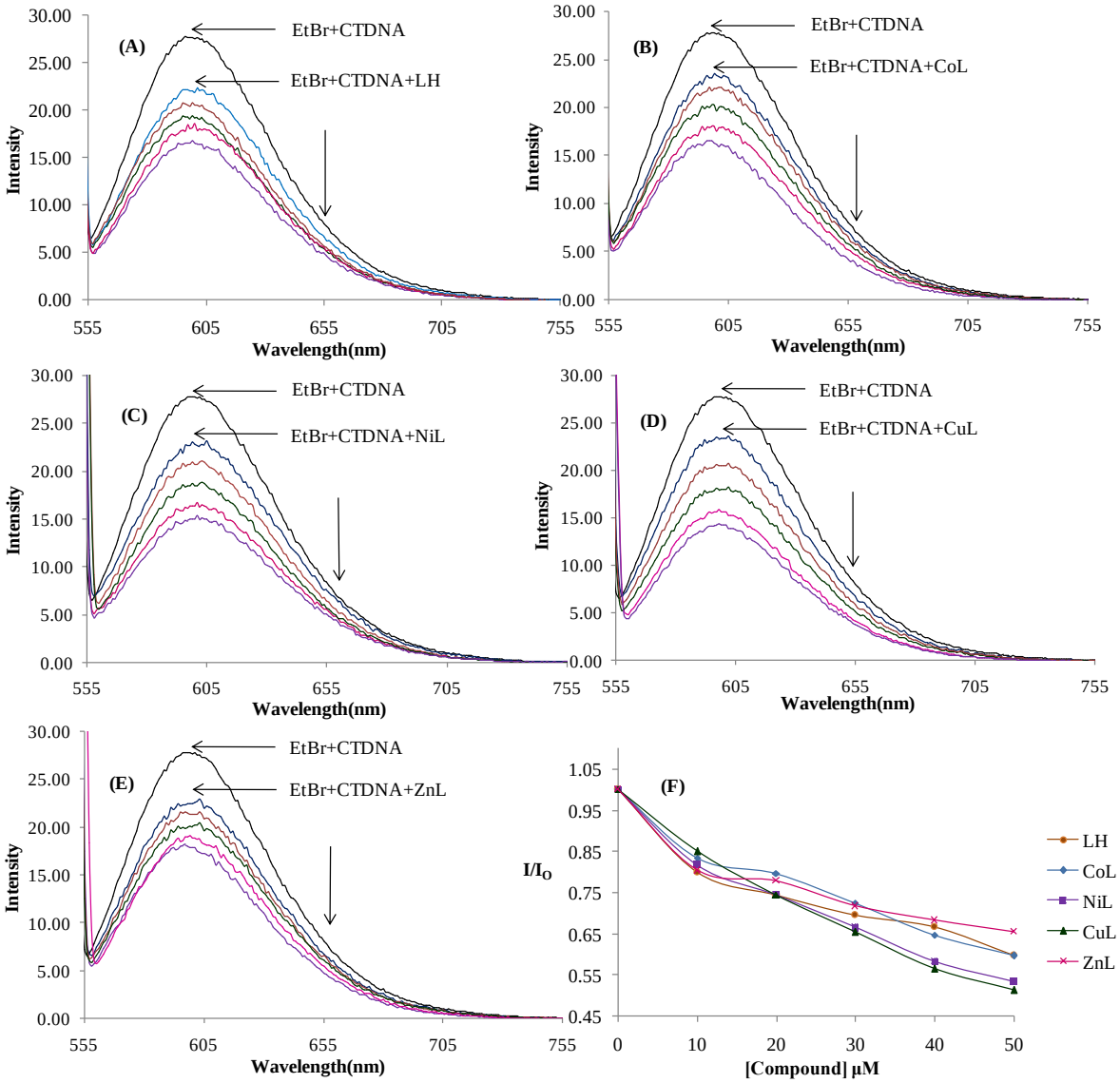

Figure 11: Effect of addition of LH(A), CoL(B), NiL(C), CuL(D), ZnL(E) on the emission intensity of the CTDNA bound ethidium bromide(20uM) at different concentrations in phosphate buffer. (F) Plots of relative integrated emission intensity versus [DNA]/[Compound] for LH, CoL, NiL, CuL and ZnL.

Viscosity Measurements

Absorption and emission studies generally provide necessary, but not sufficient clues to support interacalative binding mode. To further clarify the nature of interaction between the complexes and DNA, viscosity measurements have been carried out. Lengthening of DNA helix occurs on intercalation as base pairs are separated to accommodate the binding ligand leading to increase in DNA viscosity [23]. Partial or on classical intercalation of ligand may bend or kink the DNA helix, thereby decreasing its effective length and subsequently viscosity. The values of relative specific

viscosities of DNA in the absence and presence of complexes are plotted against [complex]/[DNA]. The relative viscosities of CT-DNA bound to ligand and its complexes, increased with increasing concentration (Figure 12), indicative of a classical intercalation [24]. The increased degree of viscosity which may depend on the binding affinity of compounds to CT-DNA follows the order CuL>CoL>NiL>LH>ZnL.

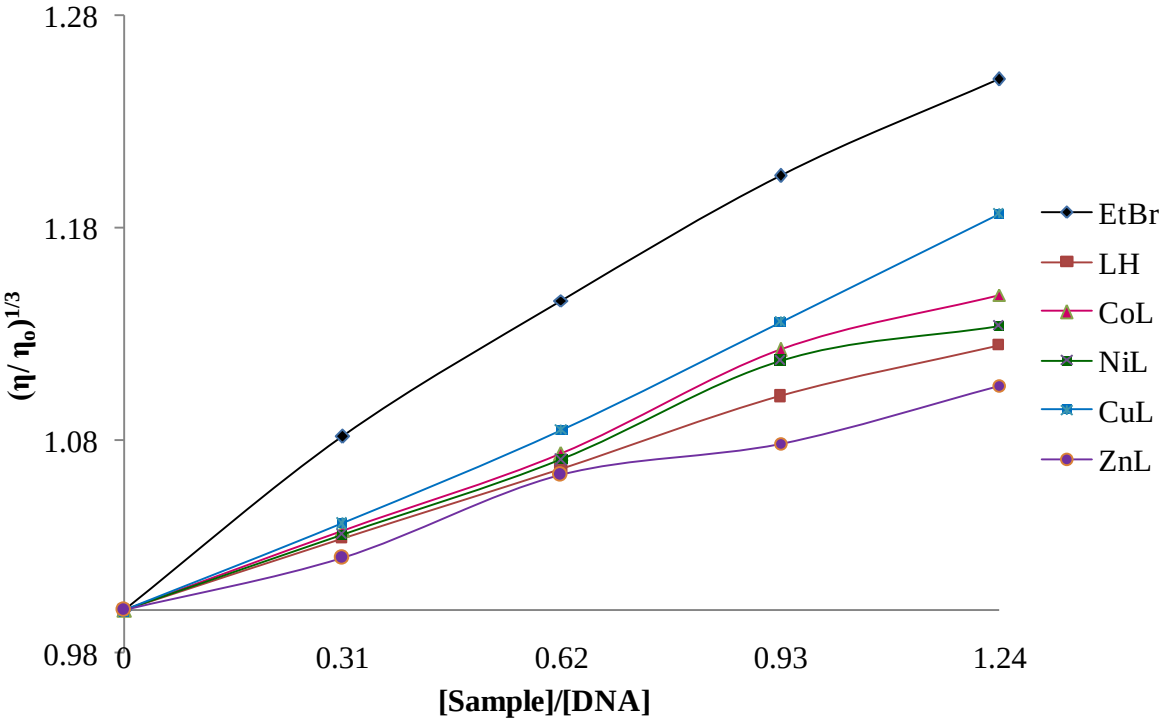

Figure 12: Effect of increasing amount of the EtBr, LH, CoL, NiL, CuLand ZnL on the relative viscosities of CTDNA at 28°C, [DNA]=200uM. The results are the mean of three independent experiments carried out under identical conditions.

DNA Cleavage Studies

The extent to which the newly synthesized ligands and their metal complexes could function as DNA cleavage agents is examined using supercoiled (SC) plasmid pBR322 DNA as a target. The agarose gel electrophoresis method employed to study the efficiency of cleavage by the synthesized compounds. The photograph representing the cleavage of DNA by various samples is presented in Figure 13.

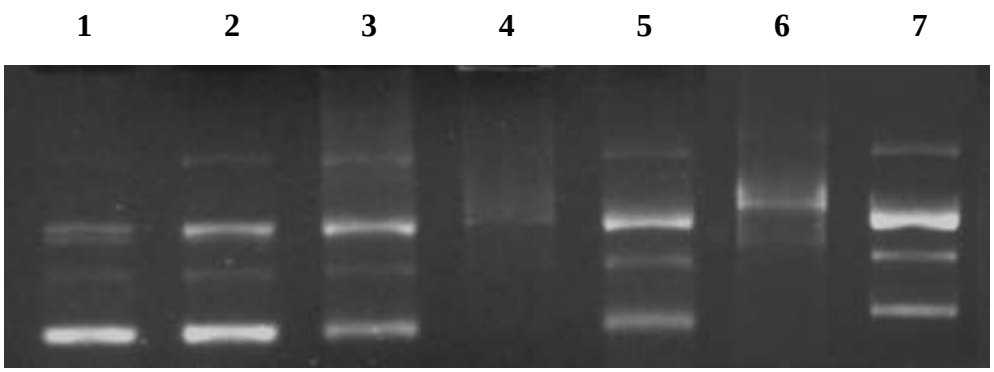

Figure 13: Lane 1, DNA (pBR322) control; Lane2, DNA+ Solvent; Lane3, DNA+L12 (100uM); Lane4, DNA+CoL (100uM); Lane5, DNA+NiL (100uM); Lane6, DNA+CuL (100uM); Lane7, DNA+ZnL (100uM).

The characterization of DNA recognition by transition metal complex has been aided by the DNA cleavage chemistry that is associated with redox-active or photoactivated metal complexes. The electrophoretic analysis clearly reveals that the new molecule and their metal complexes have acted on DNA as there has been a difference in molecular weight between the control and the treated DNA samples. Usually the pBR 322 plasmid shows nicked/open circular, linear and supercoiled DNA bands [25-26]. It is observed that at a given concentration, there is diminishing of these bands with a prominent streak when treated with the complexes compared to standard. The data clearly suggest that, DNA cleavage activity for CuL and CoL are more compared to ligand and other compounds have not shown any significant cleavage. The average activity is observed for NiL and ZnL.

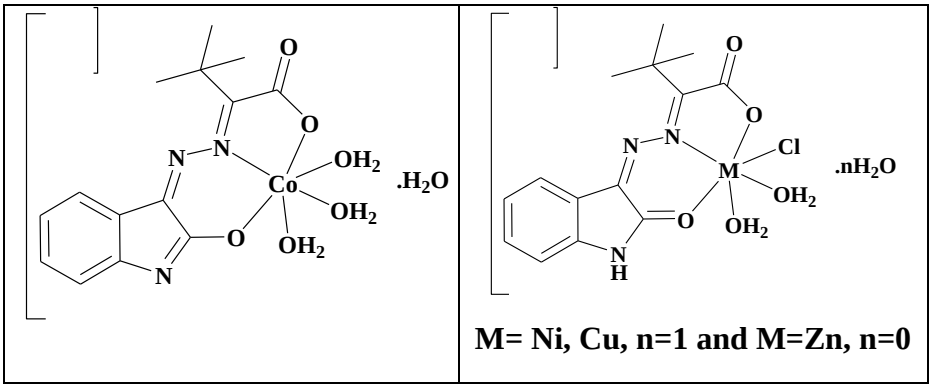

Figure 13: Tentatively assigned structures of complexes

CONCLUSION

A novel ligand (2Z,2Z)-3,3-dimethyl-2-(2-(2-oxoindolin-3-ylidene)hydrazono)butanoic acid was synthesized and characterized with various spectroscopic and analytical techniques. The ligand has exhibited tridentate coordination behavior in all metal complexes. The mode of coordination of the ligand and the tentative structures for the complexes synthesized were depicted in Figure 14.

Ligand and its metal complexes are screened for DNA interaction studies. The intercalative mode of binding to DNA is confirmed by absorption, emission, thermal denaturation and viscosity studies. The DNA binding ability of the ligands and complexes were assessed by absorption spectra and viscosity measurements, indicating that the ligands and complexes bind to DNA via intercalation. The complexes also promote cleavage of calf thymus DNA by hydrolytic mechanism. These results help to understand the mechanism of interactions of the compounds binding to DNA and helpful in the development of their potential biological, pharmaceutical and physiological implications in the future.

ACKNOWLEDGEMENT

The authors thank the USIC, Karnatak University, Dharwad for providing the spectral facilities and thankful to UGC for providing UGC-UPE fellowship and UPE-FAR-I program. Authors are thankful to Dr. V. Shyamkumar and Mrs. Delicia A. Baretto in helping gel electrophoresis.

REFERENCES

1. Sangeeta KR, Blessy BM, Sudhamani CN, Bhojya SH, Mechanism of DNA binding and cleavage. Biomedicine and Biotechnology 2014; 2,1: 1-9.
2. Cane A, Tournaire, MC. Barritault D, Crumeyrolle-Arias M. The Endogenous Oxindoles 5-Hydroxyoxindole and Isatin Are Antiproliferative and Proapoptotic. Biochem Biophys Res Commun. 2000; 276: 379.
3. Vine KL, Locke JM, Ranson M, Pyne SG, Bremner. In vitro cytotoxicity evaluation of some substituted isatin derivatives. J B Bioorg Med Chem. 2007; 15: 931.
4. Singh GS, Singh T, Lakhan R. Synthesis, C-13 NMR and anticonvulsant activity of new isatin-based spiroazetidinones. Indian J Chem. 1997; 36B: 951.
5. Verma M, Pandeya SN, Singh KN, James PS. Acta Pharm. 2004; 54: 49.
6. Pandeya SN, Yogeeshwari P, Sriram D, Nath G. Indian J Pharm Sci. 2002; 64: 209.
7. Selvam P, Murugesh N, Chandramohan M, Debyser Z, Witvroum M. Indian J Pharm Sci. 2008; 70: 779.
8. Seshaiah KS, Atmakuru R. Synthesis pharmacological activities of hydrazones, Schiff and mannich bases of isatin derivatives. Biol Pharm Bull. 2001; 24: 1149-1152.
9. Kallin H, Yao Z, Fengxi L, Qiannan G et al., Design, synthesis and in vitro cytotoxicity evaluation of 5-(2-carboxyethenyl)isatin derivatives as anticancer agents. Bioorg Med Chem Lett. 2014; 24: 591-594.

10. Satish SB, Anupa AK, Hussain H, Ayesha AK, Vivekanand VG, Shridhar PG, Vedavati GP. Synthesis, electronic structure, DNA and protein binding, DNA cleavage and anticancer activity of fluorophore-labeled Copper (II) complexes. Inorg Chem 2011; 50: 545-558.
11. Mohan NP, Promise AD, Bhupesh SB. DNA interaction, free radical scavenging and in-vitro antibacterial activity of drug-based copper (II) complexes. Appl Organometal Chem. 2011; 25: 653-660.
12. Rabindra RP, Raju N, Raghavaiah P, Hussain S. Picolinic acid based Cu(II) complexes with heterocyclic bases - crystal structure, DNA binding and cleavage studies. Eur J Med Chem 2014; 79: 117-127.
13. Archika B, Avinash K, Menakshi B, Bimba J, Ray B, Uddhavesh S, Rajendra J. Mixed-ligand copper (II) maltolate complexes: synthesis, characterization, DNA binding and cleavage, and cytotoxicity. Inorg Chem. 2009; 48: 9120-9132.
14. Aishakhanam HP, Kalagouda BG. Transition metal complexes of novel ethyl pyruvate hydrazones as potential antitumor agents: synthesis and physicochemical properties, DNA interactions and antiproliferative activity. Med Chem Res 2013; 22: 1504-1516.
15. Mosses L, Andrea LR, Michael DW, Stephen F, John AH. (GC base sequence recognition by oligo(imidazolecarboxamide) and C-terminus-modified analogues of distamycin deduced from circular dichroism, proton nuclear magnetic resonance, and methidiumpropyl ethylene diamine tetraacetate-iron (II) foot printing studies). Biochemsirty. 1993; 2: 4237-4245.
16. Nakamoto K. Infra red spectra of inorganic and coordination compounds, 2nd ed., New York; John Wiley and Sons; 1997; 171-173.
17. Pavia DL, Lampman GM, Krizand GS, Vyvyan JR. Introduction to Spectroscopy. Bellingham, Washington. 2007; 102-153.
18. G. Wilkinson, R. D. Gillard, J. A. McCleverty, "Comprehensive Coordination Chemistry". First Edn Pergamon press Oxford, 1987; 5.
19. Satyanarayana DN. Electronic absorption spectroscopy and related techniques. Hyderabad, India. 2001; 238-295.
20. N. Nawar, N. M. Hosny, Transition metal complexes of 2-acetylpyridine o-hydroxybenzoylhydrazone (APo-OHBH): their preparation, characterisation and antimicrobial activity. Chem Pharm Bull. 1999; 47: 944.

21. Z. H. Chohan, H. Pervez, A. Rauf, K. M. Khan, C. T. Supuran. Isatin-derived antibacterial and antifungal compounds and their transition metal complexes. J Enz Inhib Med Chem. 2004; 19: 417-423.
22. Azza AAAH. Synthesis and spectroscopic studies on ternary bis-Schiff-base complexes having oxygen and/or nitrogen donors. J Coord Chem. 2006; 59: 157-176.
23. Xiao-Wen L, Yong-Jun Z, Yan-Tuan L, Zhi-Yong W, Cui-Wei Y. Synthesis and structure of new bicopper(II) complexes bridged by N-(2- aminopropyl)-N0-(2-oxidophenyl)oxamide: The effects of terminal ligands on structures, anticancer activities and DNA-binding properties. Eur J Med Chem. 2011; 46: 3851.
24. Kumar CV, Emma HA. DNA binding studies and site selective fluorescence sensitization of an anthryl probe. J Am ChemSoc 1993; 115: 8547-8553.
25. Yanping L, Yanbo W, Jing Z, Pin Y. DNA-binding and cleavage studies of novel binuclear copper(II) complex with 1,10-dimethyl-2,20-biimidazole ligand. J Inorg Biochem. 2007; 101: 283-290.
26. Uma V, Kanthimathi M, Weyhermuller T, Nair BU. Oxidative DNA cleavage mediated by a new copper (II) terpyridine complex: Crystal structure and DNA binding studies. J Inorg Biochem. 2005; 99: 2299-2307.